



**HAL**  
open science

## An experimental and theoretical study of the valence shell photoelectron spectrum of bromochlorofluoromethane

D M P Holland, a W Potts, L Karlsson, I Novak, I L Zaytseva, a B Trofimov, E V Gromov, J Schirmer

► **To cite this version:**

D M P Holland, a W Potts, L Karlsson, I Novak, I L Zaytseva, et al.. An experimental and theoretical study of the valence shell photoelectron spectrum of bromochlorofluoromethane. *Journal of Physics B: Atomic, Molecular and Optical Physics*, 2010, 43 (13), pp.135101. 10.1088/0953-4075/43/13/135101 . hal-00569804

**HAL Id: hal-00569804**

**<https://hal.science/hal-00569804>**

Submitted on 25 Feb 2011

**HAL** is a multi-disciplinary open access archive for the deposit and dissemination of scientific research documents, whether they are published or not. The documents may come from teaching and research institutions in France or abroad, or from public or private research centers.

L'archive ouverte pluridisciplinaire **HAL**, est destinée au dépôt et à la diffusion de documents scientifiques de niveau recherche, publiés ou non, émanant des établissements d'enseignement et de recherche français ou étrangers, des laboratoires publics ou privés.

## An experimental and theoretical study of the valence shell photoelectron spectrum of bromochlorofluoromethane

D.M.P. Holland<sup>1</sup>, A.W. Potts<sup>2</sup>, L. Karlsson<sup>3</sup>, I. Novak<sup>4</sup>, I.L. Zaytseva<sup>5</sup>, A.B. Trofimov<sup>5,6</sup>, E.V. Gromov<sup>5,7</sup> and J. Schirmer<sup>7</sup>

<sup>1</sup> Daresbury Laboratory, Daresbury, Warrington, Cheshire WA4 4AD, UK

<sup>2</sup> Department of Physics, King's College, Strand, London WC2R 2LS, UK

<sup>3</sup> Department of Physics, Uppsala University, Box 530, SE-751 21 Uppsala, Sweden

<sup>4</sup> Department of Chemistry, National University of Singapore, Singapore 0511

<sup>5</sup> Laboratory of Quantum Chemistry, Irkutsk State University, 664003 Irkutsk, Russia

<sup>6</sup> Favorsky Institute of Chemistry, SB RAS, 664033 Irkutsk, Russia

<sup>7</sup> Theoretische Chemie, Physikalisch-Chemisches Institut, Universität Heidelberg, Im Neuenheimer Feld 229, D-69120 Heidelberg, Germany

### Abstract

The complete valence shell photoelectron spectrum of bromochlorofluoromethane (CHFCIBr), covering the binding energy range ~10-50 eV, has been recorded using synchrotron radiation and the observed structure has been interpreted using ionization energies and relative spectral intensities computed using the third-order algebraic-diagrammatic-construction (ADC(3)) scheme for the one-particle Green's function and the outer valence Green's function (OVGF) method. The theoretical results demonstrate that the inner valence region of the photoelectron spectrum is dominated by satellite structure. Angle resolved photoelectron spectra, recorded at selected excitation energies, have enabled the orbital assignments for the outer valence bands to be confirmed. The four outermost photoelectron bands, ascribed to the two pairs of orbitals associated with the nominally chlorine and bromine lone-pairs, exhibit characteristic angular distributions. The photon energy dependent variations in the relative photoelectron band intensities provide additional support for the orbital assignments.

## 1. Introduction

Bromochlorofluoromethane is one of the simplest chiral molecules possessing an asymmetric carbon atom and, as such, its geometric and electronic structure have attracted considerable interest [1-6]. Although the molecule contains two relatively heavy atoms, its size is sufficiently small for its physical properties to be calculated reliably using advanced theoretical and computational approaches. Moreover, techniques have been developed which enable a sample having enantiomeric excess to be prepared [7], thereby rendering CHFCIBr amenable to spectroscopic studies of optical activity [8]. A characterisation of the molecular orbital configuration of bromochlorofluoromethane is therefore timely.

The outer valence shell electronic structure of CHFCIBr has been investigated previously using HeI [5,6] and HeII [5] excited photoelectron spectra. The observed bands were assigned through comparison with similar structure in related molecules, the expected photon energy dependent variation in relative intensities, and calculated ionization energies and vibrational frequencies [5]. Interestingly, the four outermost bands ( $\tilde{X}$ ,  $\tilde{A}$ ,  $\tilde{B}$  and  $\tilde{C}$ ) were ascribed to ionization from essentially Br ( $\tilde{X}$  and  $\tilde{A}$ ) and Cl ( $\tilde{B}$  and  $\tilde{C}$ ) lone-pair orbitals, with each pair being split as a result of spin-orbit coupling and spatial interactions between orbitals located on different halogen atoms and/or  $\sigma$ -bonding orbitals. Ionization from the more tightly bound F lone-pair orbitals leads to a negligible spin-orbit splitting which cannot be resolved experimentally. Apart from the photoelectron bands associated with the Br and Cl lone-pairs, the assignments for the outer valence structure of CHFCIBr are not well established, and a proper interpretation of the features occurring in the inner valence region, where electron correlation becomes important, has not been proposed.

The aim of the present work is to establish the electronic structure for the entire valence shell of bromochlorofluoromethane through a comparison between vertical ionization energies and relative spectral intensities computed using the third-order algebraic-diagrammatic-construction (ADC(3)) approximation for the one-particle Green's function [9-13] and angle resolved photoelectron spectra recorded at various excitation energies. Mulliken atomic populations have also been calculated, and these have allowed those molecular orbitals

possessing a significant atomic content to be identified. This, in turn, can be correlated with the energy dependent behaviour of the associated photoelectron angular distributions and photoionization cross sections.

The photoionization dynamics of halogen containing molecules have proved particularly interesting because experimental studies have shown that the photoionization cross sections and the photoelectron asymmetry parameters associated with molecular orbitals possessing a strong halogen character exhibit atomic-like behaviour. For example, measurements on the hydrogen halides [14,15] showed that the asymmetry parameter for the outermost  $n\rho\pi$  orbital ( $n=3,4$  for Cl, Br, respectively), of essentially lone-pair character, displayed a minimum which resembled that observed in studies on the closely related rare gas atoms [16]. In  $\text{CH}_3\text{Cl}$ , the experimentally determined minimum in the  $(2e)^{-1} \tilde{X}^2E$  state asymmetry parameter at a photon energy of 41 eV has been interpreted as a Cooper minimum in the  $l=2$  channel [17]. Similarly, the dip observed around 65 eV in the  $(5e)^{-1} \tilde{X}^2E$  state asymmetry parameter of  $\text{CF}_3\text{Br}$  [18] has been attributed to the Br Cooper minimum, predicted to occur near this energy [19]. The influence of Cooper minima on essentially lone-pair orbitals in larger halogen containing molecules, such as the halobenzenes [20-22], the halothiophenes [23-25] and the halouracils [26] has also been demonstrated. Thus, angle resolved photoelectron spectra of  $\text{CHFCIBr}$ , measured in the vicinity of a Cooper minimum, should enable molecular orbitals retaining a significant halogen atom content to be identified. Furthermore, spectra recorded over a range of excitation energies will allow the photon energy dependent variations in the relative photoelectron band intensities to be determined. These variations can then be compared with those predicted from the appropriate theoretical atomic photoionization cross sections [27], thereby providing an additional guide to orbital assignment.

## 2. Experimental apparatus and procedure

The photoelectron spectra were recorded using a rotatable hemispherical electron energy analyser and synchrotron radiation emitted by the Daresbury Laboratory storage ring. Detailed descriptions of the spherical grating monochromator [28] and the experimental

procedure [29] have been reported. For the present investigation on CHFCIBr, the monochromator entrance and exit slits were adjusted to give a photon bandwidth varying from about 50 meV at 20 eV to 100 meV at 80 eV.

The photoionization differential cross section in the electric dipole approximation, assuming randomly oriented targets and electron analysis in a plane perpendicular to the photon propagation direction, can be expressed in the form

$$\frac{d\sigma}{d\Omega} = \frac{\sigma_{\text{total}}}{4\pi} \left[ 1 + \frac{\beta}{4} (3P \cos 2\theta + 1) \right]$$

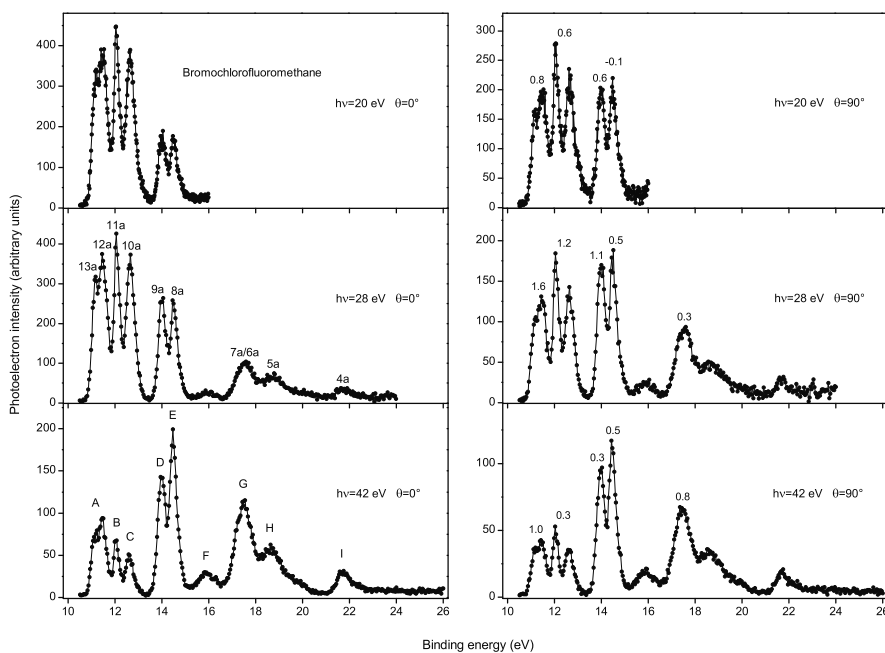
where  $\sigma_{\text{total}}$  is the angle integrated cross section,  $\beta$  is the photoelectron asymmetry parameter,  $\theta$  is the photoelectron ejection angle relative to the major polarization axis and  $P$  is the degree of linear polarization of the incident radiation. At each photon energy, photoelectron spectra were recorded at  $\theta=0^\circ$  and  $\theta=90^\circ$ , thus allowing the asymmetry parameter to be determined once the polarization had been deduced. The degree of linear polarization was determined by recording Ar 3p and He 1s photoelectron spectra as a function of photon energy, and using the well-established  $\beta$ -parameters for these gases [28].

The transmission efficiency of the analyser was determined in the usual manner by monitoring the total electron count as a function of photon energy, and hence photoelectron energy, for an inert gas. Argon photoelectron spectra were recorded for electron energies varying from approximately threshold to 100 eV. By combining these results with the total absorption cross section [30,31], and taking into account the contributions from higher order radiation [28], the transmission efficiency of the analyser could be evaluated.

Photoelectron spectra of CHFCIBr were recorded at selected photon energies and Figure 1 shows those measured at 20, 28 and 42 eV. The values of the  $\beta$ -parameters for the principal peaks are included in Figure 1 and listed in Table 1. Figure 2 displays the outer valence shell photoelectron spectrum, recorded at a photon energy of 37 eV, with improved statistics. All the spectra shown in Figures 1 and 2 have been corrected for the transmission efficiency of the analyser. Although the binding energy range spanned by the photoelectron spectra recorded at photon energies of 37 and 42 eV encompasses that in which bands J and K appear

at high photon energies, these two bands are not observed at  $h\nu=37$  or  $42$  eV because the relevant photoionization partial cross sections are small close to threshold.

The racemic mixture of CHFCIBr was prepared as described by Novak et al [5].



### 3. Computational details

The vertical ionization energies and relative spectral intensities of CHFCIBr were computed using the ADC(3) approximation scheme for the one-particle Green's function [9-13]. Both the Dyson expansion [9-11] and the non-Dyson (nD) [12,13] variants of the ADC(3) method were employed. In the latter case, calculations were performed using the so-called ADC(3/2) scheme, which treats ionization energies and intensities (pole strengths) through third and second order of many-body perturbation theory, respectively [12,13]. The present theoretical spectrum was calculated at the fixed ground-state equilibrium geometry of CHFCIBr. Of course, calculations employing relaxed final-state geometries would allow information on adiabatic transitions, and also possibly on the vibronic structure affecting the photoelectron bands, to be obtained.

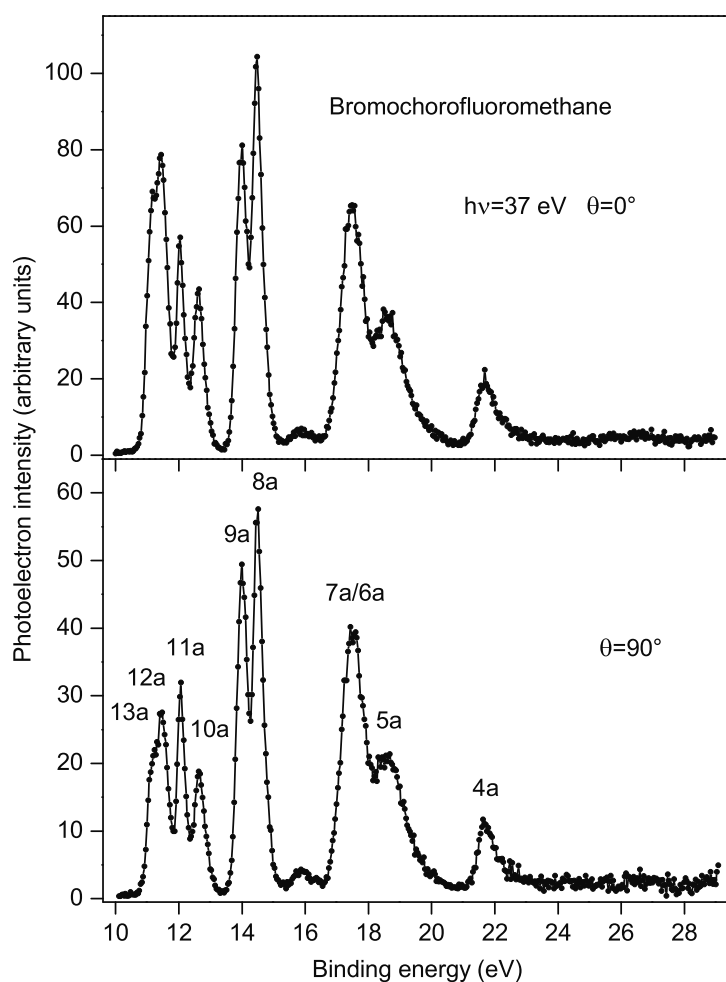
An efficient block-Lanczos iterative procedure was used to solve the ADC(3) eigenstate problem [32,33]. This method provides a very fast generation of convergent photoelectron profiles which are suitable for a reliable interpretation of the experimental data, prior to the full convergence of the individual states. This is especially useful in the description of the inner valence regions of the photoelectron spectra which are dominated by dense structure due to weak satellite transitions. Such structure is hardly accessible to most other diagonalization techniques. The specific choice of the block-Lanczos starting vectors in the form of the  $n$  unit vectors, defined within the space of 1h- (one-hole) configurations of interest, enables convergence to states with non-zero intensities. The present block-Lanczos algorithm is formulated so that only the first  $n$  rows of the eigenvectors need to be evaluated and stored [32], thereby substantially decreasing the computational efforts. In our calculations, the energies and relative intensities of the outer valence ionization transitions were iterated until full convergence was achieved. This was checked against the results of the block-Davidson diagonalization approach [34].

For the low-lying transitions, the convergence of the results with respect to choice of basis set was studied at the level of the outer valence Green's function (OVGF) approximation scheme [9,35-37]. The consistency of the present description for this low energy spectral range was checked by comparison with results obtained using the symmetry-adapted cluster configuration interaction (SAC-CI) method at the SDT (single, double, and triple excitations) level [38-42].

The calculations were performed at the equilibrium ground-state geometry of CHFCIBr, which was obtained by a full geometry optimization using the second-order Møller-Plesset (MP2) perturbation theory and the 6-311G\*\* basis set [43,44]. The calculated geometrical parameters, listed in Table 2, are essentially consistent with results obtained at the more demanding CCSD (coupled cluster singles and doubles) level using the 6-311G\*\* basis set.

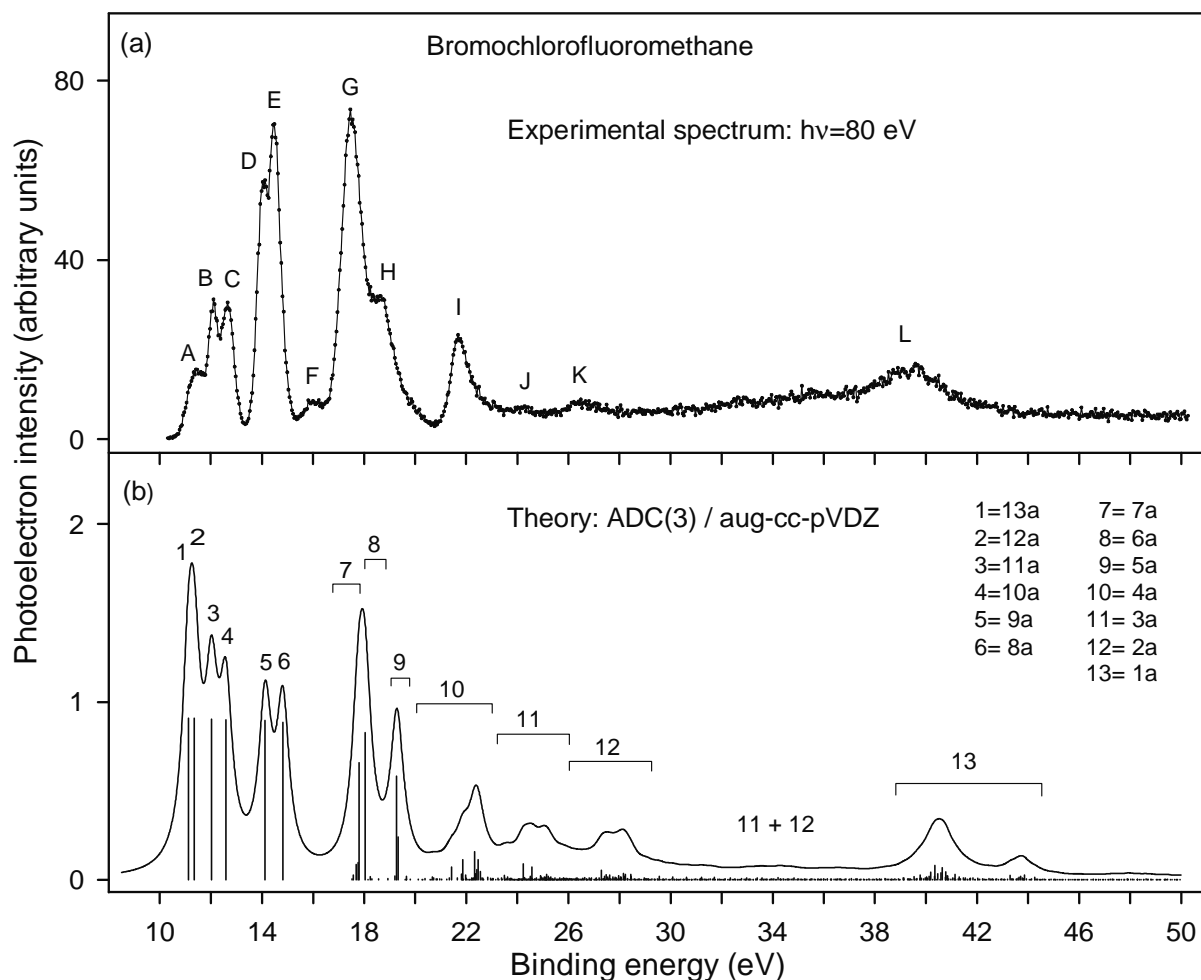
Several basis sets were employed in the present work. For the OVGF calculations these comprised the 6-311G\* and 6-311++G\*\* basis sets [43,44], the correlation consistent

polarized valence double-, triple-, quadruple- and pentuple- $\zeta$  basis sets (cc-pVDZ, cc-pVTZ, cc-pVQZ and cc-pV5Z, respectively), as well as their augmented counterparts (aug-cc-pVDZ, aug-cc-pVTZ and aug-cc-pVQZ, respectively) [45-47]. The aug-cc-pVDZ basis set was used in our ADC(3) calculations, while the cc-pVDZ basis set was used in the SAC-CI (SDT) calculations. The Cartesian representation of basis functions was used in the ADC(3) calculation. The diffuse polarization functions were omitted. All our calculations adopted the frozen-core approximation.



The (Dyson-expansion) ADC(3) and the nD-ADC(3) calculations were performed using the original codes [48,49] linked to the GAMESS ab initio program package [50]. The MP2,

CCSD, OVGf and SAC-CI(SDT) calculations were carried out using the GAUSSIAN package of programs [51].



The theoretical photoelectron spectrum (Figure 3) was constructed by convoluting the ADC(3) results for individual transitions with Lorentzians of 0.6 eV (FWHM). This convolution takes into account, in an approximate manner, both the experimental resolution (50-100 meV) and the vibrational envelopes (a few hundred meV) associated with the individual transitions. The construction does not take into account differences in the partial photoionization cross sections associated with the various molecular orbitals. Thus, whilst the agreement between the experimental and theoretical binding energies is good, the match between the observed and predicted photoelectron band intensities is less satisfactory.

#### 4. Results and discussion

The ground-state Hartree-Fock (HF) electronic configuration of bromochlorofluoromethane can be written as

Inner valence:  $1a^2 2a^2 3a^2 4a^2 5a^2$

Outer valence:  $6a^2 7a^2 8a^2 9a^2 10a^2 11a^2 12a^2 13a^2$

where core orbitals formed from all the K-shell atomic orbitals and the L- and M-shell orbitals of chlorine and bromine are not included in this description. The highest occupied molecular orbitals (MOs), 10a through to 13a, can be characterised as halogen lone-pairs derived from the p-type atomic orbitals (AOs) of bromine (MOs 12a and 13a) and chlorine (MOs 10a and 11a). This is supported by the present Mulliken population analysis given in Table 3. The F 2p atomic orbitals lie at higher binding energies and are more strongly involved in the bonding with the central carbon atom. According to our results, the corresponding orbitals (7a and 6a) show pronounced carbon, chlorine and bromine character in addition to fluorine character. This is in agreement with the previous assignment of the CHFCIBr orbitals given by Novak et al [5]. The principal carbon-halogen bonding orbitals are 9a (having increased chlorine and bromine character), 8a (having increased fluorine and chlorine character) and 5a (having nearly pure carbon-fluorine character). Our characterisation of the 8a and 9a orbitals disagrees with that inferred by Novak et al [5]. Whereas the semiempirical arguments used by Novak et al attribute C-F/C-Cl and C-H/C-Br character to the 8a and 9a orbitals, respectively, our Mulliken population analysis indicates that the 8a orbital is C-F, C-Cl and C-H bonding while the 9a orbital possesses C-Br, C-Cl and C-F bonding character. The 5a orbital is shown to possess almost exclusively carbon and fluorine character and is presumably C-F bonding with possible fluorine lone-pair character. The remaining orbitals, 4a through to 2a, are inner valence orbitals with varying amounts of C-X bonding (X=H, F, Cl, Br), possessing mixed halogen character. The innermost 1a orbital has almost exclusively F 2s character.

The ADC(3) results are in very good agreement with the experimental data (Table 4). The agreement is excellent for the main lines corresponding to the 13a to 9a orbitals in the outer

valence region. A somewhat larger difference, of  $\sim 0.3$  eV, is found between the calculated and experimental ionization energies for the 8a orbital. However, this is still within the usual accuracy limits of the ADC(3) scheme. According to our calculations, the orbital picture of ionization breaks-down [52] for the 7a orbital where several components emerge, rather than a single ionic band. We note that the predictions of the Dyson and non-Dyson methods with respect to the energies and intensities of these transitions differ from each other. This is probably due to the subtle balance between 1h- and 2h-1p- (two-hole-one-particle) configurations associated with the 7a orbital. The next transition,  $(6a)^{-1}$ , is hardly affected by configuration interaction effects, and gives rise to a main spectroscopic line with a pole strength of 0.82. At higher energies, a comparison between the individual transitions and the experimental data is no longer feasible due to the intense satellite structure. The latter originates from ionization of the more tightly bound molecular orbitals and represents a manifestation of the break-down of the orbital picture of ionization [52].

The low-lying satellite structure associated with the 7a orbital (the lowest of the two fluorine lone-pairs) can be explained by the localization properties of this molecular orbital. As seen from Table 3, the carbon atom and all three halogen atoms contribute to the 7a MO. The corresponding 1h-state couples to the 2h-1p states, with two vacancies distributed amongst the different halogen atoms and an electron excited into one of the virtual MOs localised near the central carbon atom.

The present OVGf results are also in good agreement with the measurements (Table 5). Interestingly, the OVGf ionization energies tend to overshoot the experimental values as the basis is improved, with the energies increasing as the basis set is augmented by higher polarization and diffuse functions. The best agreement between experiment and theory is obtained at the aug-cc-pVDZ and cc-pVTZ levels. The ionization energies increase in both the cc-p-VXZ and the aug-cc-pVXZ series (X=D, T, Q, 5), apparently reaching convergence for the outermost orbitals only beyond the cc-pVQZ level. The aug-cc-pVQZ and cc-pV5Z basis sets yield nearly identical results. It should be noted that in the latter OVGf calculations the 456 contracted basis functions were used. The observed slow convergence of

the ionization energies, with respect to basis set size, is probably due to the heavy atoms for which the choice of an adequate basis set is a demanding task. The present results indicate that in the complete basis set limit the vertical OVGf ionization energies for the lowest five transitions will be about 0.2 eV above the present experimental values. This can be considered as a very satisfactory agreement between theory and experiment. The remaining discrepancy is obviously due to higher-order electron correlation, vibrational effects and possibly relativistic effects, all of which should be important in CHFCIBr. The influence of higher-order electron correlation effects on the theoretical results is confirmed by the observation that the ionization energies obtained using the theoretically more rigorous ADC(3) treatment are systematically lower than the OVGf values by 0.1 eV. A similar improvement can be expected for the basis set converged results in going from the OVGf to the ADC(3) level of theory. Finally we note that the 6-311G\*\*, 6-311++G\*\* and cc-pVDZ basis sets yield similar ionization energies, which are uniformly ~0.5 eV below their converged values.

The present theoretical results allow the photoelectron spectrum of bromochlorofluoromethane to be assigned in the energy range up to ~50 eV (Figure 3, and Tables 4 and 5), with the generated spectral profile qualitatively reproducing all the features appearing in the experimental spectrum.

According to our calculations, the overlapping bands observed in the experimental spectrum in the binding energy range ~10.5-13.5 eV accommodate four transitions (Table 4 and Figure 3). Peaks B and C, at binding energies of 12.02 and 12.62 eV, can be attributed readily to the  $(11a)^{-1}$  and  $(10a)^{-1}$  transitions, respectively, corresponding to the chlorine lone-pair orbitals. The broad doublet A, with maxima at 11.15 and 11.43 eV (Figures 1 and 2) encompasses two closely spaced transitions,  $(12a)^{-1}$  and  $(13a)^{-1}$ , associated with the bromine lone-pairs. These assignments for the four outermost bands of CHFCIBr are similar to those proposed by Novak et al [5] and by Mathis et al [6].

Support for the lone-pair assignments proposed for bands A, B and C is obtained from the associated  $\beta$ -parameters and from the photon energy dependent relative intensity variations. Consider, first, the  $\beta$ -parameters for these bands, listed in Table 1. If the molecular orbital associated with each of the bands retains a significant atomic character, as is indeed the case as demonstrated by the Mulliken atomic populations (Table 3), then the energy dependent variations in the  $\beta$ -parameters should resemble those in the corresponding atomic orbitals. The Cl 3p and Br 4p Cooper minimum are predicted to occur at  $\sim 40$  and  $\sim 65$  eV, respectively [19]. Table 1 shows that the  $\beta$ -parameter for bands (B+C), due to the nominally Cl lone-pair orbitals, has a value of 0.6 at 20 eV, rises to 1.2 at 28 eV and then dips to 0.3 at 42 eV, with the latter energy coinciding with the atomic Cooper minimum. Although this variation in the  $\beta$ -parameter is slightly less than is predicted for the atomic case, where  $\beta$  (Cl 3p)  $\sim 1.8$  at 15 eV and  $\sim 0.2$  in the Cooper minimum [19], it closely resembles the behaviour observed for essentially Cl lone-pair orbitals in chlorine containing molecules [17,20,23]. The second source of experimental support for the assignments proposed for bands B and C comes from the variation in relative intensity as a function of excitation energy. It is noticeable that peaks B and C change from being the most intense in the spectra recorded at 20 and 28 eV, to being relatively weak in that recorded at 42 eV. This variation is readily understood through consideration of atomic photoionization cross sections. Photoelectron bands D, E, G and H (Figure 3) arise from orbitals containing at least some fluorine contribution (Table 3). The theoretical photoionization cross section for F 2p decreases only marginally between 21 and 41 eV, whereas that for Cl 3p changes from  $\sim 47$  Mb at 17 eV to  $\sim 0.6$  Mb at 41 eV [27]. Thus the observed behaviour in the relative peak intensities provides further evidence for the Cl lone-pair assignment for peaks B and C.

Similar arguments can be made for associating doublet A with the Br lone-pair orbitals. Table 1 shows that the  $\beta$ -parameter for band A reaches a maximum of 1.6 at 28 eV and then decreases. Analysis of a photoelectron spectrum recorded at 55 eV (not shown), near to the energy predicted for the Br 4p Cooper minimum, indicates that  $\beta \sim 0.0$ . This variation in the  $\beta$ -value with photon energy closely resembles that calculated for the Br 4p atomic orbital,

where  $\beta \sim 1.9$  at 30 eV and then drops to approximately zero in the Cooper minimum. It also closely resembles the variations observed for essentially Br 4p lone-pair orbitals in bromine containing molecules [21,24]. The photon energy dependent relative intensity variations of band A provides additional confirmation for the Br lone-pair assignment because the Br 4p atomic photoionization cross section is calculated to decrease from  $\sim 39$  Mb at 17 eV to  $\sim 1$  Mb at 41 eV [27].

Bands D and E (Figure 3), with maxima at 13.98 and 14.46 eV, are due to the  $(9a)^{-1}$  and  $(8a)^{-1}$  transitions, respectively. As already mentioned, both of these orbitals may be characterised as carbon-halogen bonding. The Mulliken atomic population for the 8a orbital shows that the highest contribution arises from the F atom and that the C atom also contributes significantly. The Mulliken atomic population for the 9a orbital is similar to that for the 8a orbital although the F atom content is somewhat reduced. These atomic populations, when combined with the theoretical atomic photoionization cross sections, readily explain the increase in relative intensity of bands D and E, when compared to the lone-pair bands, at higher photon energies. The relevant calculated photoionization cross sections at 21.2 and 40.8 eV are: 6.1 and 1.9 Mb (C 2p), 9.3 and 8.4 Mb (F 2p), 13.9 and 0.6 Mb (Cl 3p), and 15.6 and 1.0 Mb (Br 4p) [27]. Thus, the photoelectron bands associated with molecular orbitals containing significant F 2p and/or C 2p content would be expected to become relatively more prominent than those containing a significant Cl 3p or Br 4p content as the photon energy increases. Interestingly, bands D and E have approximately equal intensity close to threshold (Figure 1) whereas at higher energy (Figure 3) band E is more intense than band D. This is in accord with the Mulliken atomic populations which show that the 8a orbital has a higher F 2p content than does the 9a orbital.

In our photoelectron spectrum of CHFCIBr, a small peak, labelled F, appears at a binding energy of 15.8 eV (Figure 3). The corresponding band is missing in the HeI excited spectrum [5] but a low intensity feature might be discerned in the HeII excited spectrum [5]. The interpretation of peak F presents some difficulties, and the question as to whether this peak genuinely belongs to the photoelectron spectrum of CHFCIBr will now be considered.

Since, in the ADC(3) approach, only 1h- and 2h-1p configurations are explicitly taken into account, we have performed some additional SAC-CI(SDT) calculations which include 3h-2p- (three-hole-two-particle) configurations to check the relevance of these configurations. The results of our calculations are summarised in Table 6, where the twelve lowest ionization energies obtained using the nD-ADC(3) and SAC-CI(SDT) methods are compared to the present experimental data. Neither the ADC(3) nor the SAC-CI(SDT) results show any indications of vertical transitions in the energy range 14.7-17.2 eV. The nD-ADC(3) and SAC-CI(SDT) results agree remarkably well with each other, which indicates explicitly that the 3h-2p- configurations play only a minor role in the spectral region under consideration. Thus, it is safe to conclude that peak F is not due to a vertical ionization transition.

What other possibilities remain which could explain peak F? The structure might be due to some vibronic coupling involving the ionic states arising from ionization of the 7a orbital. Also, some relativistic effect associated with the Br atom cannot be ruled out a priori as the origin of this feature. The most likely explanation, however, would appear to be that peak F is due to the presence of an impurity. Apart from the weak feature F, the spectra recorded at photon energies of 20 and 42 eV (Figure 1) are very similar to the reported HeI and HeII excited spectra [5]. It is, however, reasonable to assume that an impurity will give rise to more than one feature in the spectrum. Therefore it appears that if peak F is associated with an impurity, then any other impurity features must be as weak as, or weaker than, peak F or they would produce observable changes to the spectra. Peak F is observed at a binding energy of ~15.8 eV, which seems high for an energy corresponding to ionization from an outermost orbital and it is difficult to suggest a suitable impurity candidate. A possible explanation might be that the impurity is a result of decomposition occurring within the spectrometer system. A possible candidate might be F<sub>2</sub> [53]. Band F could then correspond to unresolved ionization from the  $1\pi_g$  orbital, peaking at 15.8 eV, while ionization from the  $1\pi_u$  orbital at 18.8 eV would be masked by overlapping with the G and H bands.

The broad bands G and H, with maxima at 17.5 and 18.6 eV, respectively, originate from ionization of the 7a, 6a and 5a orbitals. As already discussed, the 7a orbital gives rise to

extensive satellite structure which, together with the  $(6a)^{-1}$  main line, form band G. The 5a orbital and its satellites are responsible for band H. The Mulliken atomic populations (Table 3) show that the 7a and 6a orbitals contain a substantial F lone-pair contribution and that they are also C-F bonding. The 5a orbital also possesses a significant F content and is C-F and C-H bonding. The large fluorine content in these orbitals is confirmed by the relative prominence of bands G and H at high photon energy. In the photoelectron spectrum recorded at 80 eV (Figure 3), band G is the dominant peak, as would be expected based on a consideration of the energy dependence of the F 2p photoionization cross section. Moreover, the  $\beta$ -parameter for band G at 42 eV (0.8) is typical of that for molecular orbitals having a strong F 2p lone-pair character [54].

At binding energies above 21 eV, the photoelectron spectrum of CHFCIBr is formed exclusively from satellite bands associated with the inner valence levels. Within certain energy intervals, these satellite bands can be related to the orbitals from which their spectral intensity has been acquired. Band I, whose maximum is observed at 21.7 eV, can be attributed to the satellite structure originating from the 4a orbital (with a HF energy of 24.8 eV). The corresponding band in the theoretical spectrum is located between 21.1 and 23.0 eV, with its maximum being at 22.4 eV. The weak experimental maxima J and K at 24.2 and 26.4 eV, respectively, can be ascribed to satellite groups associated with the 3a (HF energy 28.88 eV) and 2a (HF energy 32.20 eV) orbitals, with strong Br and Cl character, respectively. In the theoretical spectrum, the bands due to the latter orbitals are found in the energy intervals 24.0-25.6 and 27.0-28.6 eV, with centres of gravity at  $\sim$ 24.7 and 27.7 eV, respectively.

The broad band L, located between  $\sim$ 36 and 43 eV in the experimental spectrum, with a maximum near 39.3 eV, is associated with ionization from the 1a orbital. This orbital is characterised by a HF energy of 45.5 eV and the corresponding spectral profile (Figure 3) exhibits maxima at 40.5 and 43.8 eV. As the 1a orbital corresponds essentially to the F 2s orbital, a photoelectron peak with a binding energy around 40 eV occurs in many fluorine containing molecules, for example, CF<sub>4</sub> [54], SF<sub>6</sub> [55] and SiF<sub>4</sub> [56]. However, the peak

profile and the number of separate components contributing to the structure, varies from molecule to molecule.

As can be seen from Figure 3, the energy region between 30 and 38 eV contains a continuous photoelectron intensity. According to our theoretical results, this region is filled with various satellites related to the 4a and 3a orbitals. This 'correlation tail' is probably responsible for the slight increase in the photoelectron signal, observed in the corresponding energy range, culminating in band L.

The observed disparities between the theoretical and experimental spectra at binding energies above 20 eV are not unexpected since, in the present ADC(3) treatment, bands formed by transitions to states dominated by 2h-1p- configurations are less accurately described than those due to transitions into states characterised by 1h- configurations. Whereas the latter class of configuration is treated consistently through third order, only a first order treatment applies to the 2h-1p satellite states. Thus, above 20 eV, a quantitative agreement between experiment and theory can be achieved only at the fourth order ADC(4) level employing, moreover, basis sets which are sufficiently large to properly describe the excited cationic states.

Returning now to the two pairs of bands associated with the Cl and Br lone-pair orbitals in CHFCIBr, it is evident that the splitting between the two components is larger for the Cl lone-pair than for the Br lone-pair. The atomic spin-orbit coupling parameters are 0.073 and 0.305 eV for Cl and Br, respectively [57], thus it might be anticipated that the splitting between the essentially Br lone-pair orbitals in CHFCIBr would be greater than that between the essentially Cl lone-pair orbitals, as is commonly observed in halogen containing molecules [20,21,23,24,26].

This unexpected behaviour has been discussed by Novak et al [5], specifically in regard to CHFCIBr, and more generally in connection with related chiral halomethanes [58,59]. In CHFCIBr, Novak et al [5] attributed the unusually large splitting between the nominally

Cl 3p lone-pair bands to the so-called 'CHF effect'. Based upon this interpretation, a large splitting occurs when only a single fluorine atom is present in the molecule, with the splitting arising from the electrostatic interaction between the orthogonal Cl 3p components and the attractive potential created by the highly electronegative fluorine atom.

Depending on the computational scheme, the splitting between the lone-pair orbitals in CHFClBr is calculated to be 0.2 eV for Br and 0.6-0.7 eV for Cl. This effect is the same at the HF and correlated levels of theory and, thus, reflects features of the molecular orbital level. Starting from the experimental ionization energies of Br (~11.8 eV) and Cl (~13.0 eV) [60], and using the present experimental ionization energies for the 10a-13a orbitals of CHFClBr (Table 4), it can be seen that the Br 4p and Cl 3p halogen levels experience a mean lowering of ~0.5 and 0.7 eV and a splitting of ~0.28 and 0.60 eV, respectively, as a result of molecular orbital formation. The larger chlorine energy split and shift indicate that the Cl 3p AOs are involved in molecular bonding to a greater extent than are the Br 4p AOs. The unexpected observation, however, is that the 11a orbital is shifted more distinctly to lower energy (by ~1 eV) than is the 10a orbital (~0.4 eV). Inspection of the Mulliken atomic populations reveals subtle differences between the 11a and the 10a orbitals which may explain this behaviour. In contrast to the 10a orbital, which has essentially only chlorine and a much smaller bromine character, the 11a orbital has, in addition, some carbon and hydrogen character. This indicates that the 11a orbital is more strongly involved in the bonding of these atoms. Our results do not support the interpretation of the 'CHF effect' proposed by Novak et al [5] but show that the chlorine lone-pair orbitals are integrated into the molecular environment and contribute significantly to bonding in bromochlorofluoromethane. Similar molecular arguments presumably apply to other CHF halogenated methanes where large Cl lone-pair splittings have been observed.

## **Acknowledgments**

ILZ and ABT gratefully acknowledge support from the Russian Foundation for Basic Research. EVG acknowledges support from the Deutsche Forschungsgemeinschaft.

## References

- [1] Bauder A, Beil A, Luckhaus D, Müller F and Quack M 1997 *J. Chem. Phys.* **106** 7558
- [2] Polavarapu P L 2002 *Angew. Chem. Int. Ed.* **41** 4544
- [3] Cuisset A, Aviles Moreno J R, Huet T R, Petitprez D, Demaison J and Crassous J 2005 *J. Phys. Chem.* **A109** 5708
- [4] Rauhut G, Barone V and Schwerdtfeger P 2006 *J. Chem. Phys.* **125** 054308
- [5] Novak I, Ng S C, and Potts A W 1993 *Chem. Phys. Lett.* **215** 561
- [6] Mathis J E, Compton R N, Boyles D C and Pagni R M 1996 *Mol. Phys.* **89** 505
- [7] Doyle T R and Vogl O 1989 *J. Am. Chem. Soc.* **111** 8510
- [8] Daussy Ch, Marrel T, Amy-Klein A, Nguyen C T, Bordé Ch J and Chardonnet Ch 1999 *Phys. Rev. Lett.* **83** 1554
- [9] von Niessen W, Schirmer J and Cederbaum L S 1984 *Comp. Phys. Rep.* **1** 57
- [10] Schirmer J, Cederbaum L S and Walker O 1983 *Phys. Rev.* **A28** 1237
- [11] Schirmer J and Angonoa G 1989 *J. Chem. Phys.* **91** 1754
- [12] Schirmer J, Trofimov A B and Stelter G 1998 *J. Chem. Phys.* **109** 4734
- [13] Trofimov A B and Schirmer J 2005 *J. Chem. Phys.* **123** 144115
- [14] Carlson T A, Krause M O, Fahlman A, Keller P R, Taylor J W, Whitley T and Grimm F A 1983 *J. Chem. Phys.* **79** 2157
- [15] Carlson T A, Fahlman A, Krause M O, Whitley T A and Grimm F A 1984 *J. Chem. Phys.* **81** 5389
- [16] Becker U and Shirley D 1996 in: U. Becker, D. Shirley (Eds), *VUV and Soft X-Ray Photoionization*, Plenum Press, New York, p135
- [17] Holland D M P, Powis I, Öhrwall G, Karlsson L and von Niessen W 2006 *Chem. Phys.* **326** 535
- [18] Novak I, Benson J M and Potts A W 1986 *Chem. Phys.* **104** 153
- [19] Manson S T, Msezane A, Starace A F and Shahabi S 1979 *Phys. Rev.* **A20** 1005
- [20] Potts A W, Edvardsson D, Karlsson L, Holland D M P, MacDonald M A, Hayes M A, Maripuu R, Siegbahn K and von Niessen W 2000 *Chem. Phys.* **254** 385

- [21] Holland D M P, Edvardsson D, Karlsson L, Maripuu R, Siegbahn K, Potts A W and von Niessen W 2000 Chem. Phys. **252** 257
- [22] Holland D M P, Edvardsson D, Karlsson L, Maripuu R, Siegbahn K, Potts A W and von Niessen W 2000 Chem. Phys. **253** 133
- [23] Trofimov A B, Schirmer J, Holland D M P, Karlsson L, Maripuu R, Siegbahn K and Potts A W 2001 Chem. Phys. **263** 167
- [24] Potts A W, Trofimov A B, Schirmer J, Holland D M P and Karlsson L 2001 Chem. Phys. **271** 337
- [25] Trofimov A B, Schirmer J, Holland D M P, Karlsson L, Maripuu R and Siegbahn K 2002 J. Phys. B: At. Mol. Opt. Phys. **35** 5051
- [26] Holland D M P, Potts A W, Karlsson L, Zaytseva I L, Trofimov A B and Schirmer J 2008 Chem. Phys. **352** 205
- [27] Yeh J -J 1993 Atomic Calculations of Photoionization Cross Sections and Asymmetry Parameters (Langhorne: Gordon and Breach)
- [28] Finetti P, Holland D M P, Latimer C J, Binns C, Quinn F M, Bowler M A, Grant A F and Mythen C S 2001 Nucl. Instrum. Methods **B184** 627
- [29] Holland D M P, MacDonald M A, Hayes M A, Baltzer P, Karlsson L, Lundqvist M, Wannberg B and von Niessen W 1994 Chem. Phys. **188** 317
- [30] Marr G V and West J B 1976 At. Data Nucl. Data **18** 497
- [31] Chan W F, Cooper G, Guo X, Burton G R and Brion C E 1992 Phys. Rev. **A46** 149
- [32] Meyer H -D and Pal S 1998 J. Chem. Phys. **91** 6195
- [33] The block Lanczos code originally written by H.-D. Meyer and further developed by A.B. Trofimov.
- [34] The block-Davidson code originally written by F. Tarantelli.
- [35] Zakrzewski V G and von Niessen W 1993 J. Comput. Chem. **14** 13
- [36] Zakrzewski V G and Ortiz J V 1995 Int. J. Quantum Chem. **53** 583
- [37] Zakrzewski V G and Ortiz J V 1994 Int. J. Quantum Chem. **S28** 23
- [38] Nakatsuji H and Hirao K 1978 J. Chem. Phys. **68** 2053
- [39] Nakatsuji H 1978 Chem. Phys. Lett. **59** 362

- [40] Nakatsuji H 1979 Chem. Phys. Lett. **67** 329
- [41] Nakatsuji H 1979 Chem. Phys. Lett. **67** 334
- [42] Ehara M, Ishida M, Toyota K and Nakatsuji H 2002 in: K.D. Sen (Ed), Reviews in Modern Quantum Chemistry, World Scientific, Singapore, p293
- [43] Krishnan R, Binkley J S, Seeger R and Pople J A 1980 Chem. Phys. **72** 650
- [44] Curtiss L A, McGrath M P, Blandeau J -P, Davis N E, Binning R C and Radom L 1995 J. Chem. Phys. **103** 6104
- [45] Woon D E and Dunning T H 1993 J. Chem. Phys. **98** 1358
- [46] Kendall R A, Dunning T H and Harrison R J 1992 J. Chem. Phys. **96** 6769
- [47] Dunning T H 1989 J. Chem. Phys. **90** 1007
- [48] The Dyson expansion ADC(3) code originally written by G. Angonoa, O. Walter and J. Schirmer; further developed by M.K. Scheller and A.B. Trofimov.
- [49] The nD-ADC(3) code originally written by A.B. Trofimov.
- [50] Schmidt M W, Baldridge K K, Boatz J A, Elbert S T, Gordon M S, Jensen J H, Koseki S, Matsunaga N, Nguyen K A, Su S, Windus T L, Dupuis M and Montgomery J A 1993 J. Comput. Chem. **14** 1347
- [51] Frisch M J, Trucks G W, Schlegel H B, Scuseria G E, Robb M A, Cheeseman J R, Zakrzewski V G, Montgomery J A, Stratmann R E, Burant J C, Dapprich S, Millam J M, Daniels A D, Kudin K N, Strain M C, Farkas O, Tomasi J, Barone V, Cossi M, Cammi R, Mennucci B, Pomelli C, Adamo C, Clifford S, Ochterski J, Petersson G A, Ayala P Y, Cui Q, Morokuma K, Malick D K, Rabuck A D, Raghavachari K, Foresman J B, Cioslowski J, Ortiz J V, Baboul A G, Stefanov B B, Liu G, Liashenko A, Piskorz P, Komaromi I, Gomperts R, Martin R L, Fox D J, Keith T, Al-Laham M A, Peng C Y, Nanayakkara A, Gonzalez C, Challacombe M, Gill P M W, Johnson B, Chen W, Wong M W, Andres J L, Gonzalez C, Head-Gordon M, Replogle E S, Pople J A 1998 Gaussian 98, Revision A.7, Gaussian, Inc., Pittsburgh, PA
- [52] Cederbaum L S, Domcke W, Schirmer J and von Niessen W 1986 Adv. Chem. Phys. **65** 115
- [53] van Lonkhuyzen H and de Lange C A 1984 Chem. Phys. **89** 313

- [54] Holland D M P, Potts A W, Trofimov A B, Breidbach J, Schirmer J, Feifel R, Richter T, Godehusen K, Martins M, Tutay A, Yalcinkaya M, Al-Hada M, Eriksson S and Karlsson L 2005 Chem. Phys. **308** 43
- [55] Holland D M P, MacDonald M A, Baltzer P, Karlsson L, Lundqvist M, Wannberg B and von Niessen W 1995 Chem. Phys. **192** 333
- [56] Holland D M P, Potts A W, Karlsson L, Trofimov A B and Schirmer J 2002 J. Phys. B: At. Mol. Opt. Phys. **35** 1741
- [57] Brogli F and Heilbronner E 1971 Helv. Chim. Acta **54** 1423
- [58] Novak I, Ng S C, Jin S and Potts A W 1997 J. Chem. Phys. **106** 9963
- [59] Novak I, Li D B and Potts A W 2002 J. Phys. Chem. **A106** 465
- [60] Kimura K, Katsumata S, Achiba Y, Yamazaki T and Iwata S 1981 Handbook of HeI photoelectron spectra of fundamental organic molecules (Tokyo: Japan Scientific Societies Press)

Table 1

Photoelectron asymmetry parameters for the spectra of bromochlorofluoromethane shown in Figure 1

Photon energy (eV)	Asymmetry parameter <sup>a</sup>				
	Band A	Bands (B+C)	Band D	Band E	Band G
20	0.8	0.6	0.6	-0.1	
28	1.6	1.2	1.1	0.5	0.3
42	1.0	0.3	0.3	0.5	0.8

<sup>a</sup> The experimental uncertainty is  $\sim 0.2 \beta$  units.

Table 2

Equilibrium ground-state geometrical parameters of bromochlorofluoromethane calculated at the MP2 / 6-311G\*\* and CCSD / 6-311G\*\* level of theory (bond lengths in Å, angles in degrees)

Parameter	MP2	CCSD
Bond lengths		
C-H	1.086	1.086
C-F	1.349	1.347
C-Cl	1.759	1.763
C-Br	1.935	1.940
Angles		
H-C-F	109.5	109.4
H-C-Cl	108.7	108.8
H-C-Br	107.6	107.6
F-C-Cl	109.5	109.4
F-C-Br	109.2	109.1
Cl-C-Br	112.4	112.5

Table 3

Mulliken atomic population in each molecular orbital of bromochlorofluoromethane (units are electrons; sum over all atoms is 2) computed at the HF / 6-311G\*\* level of theory

Molecular orbital	Assignment	C	H	F	Cl	Br
13a	LP Br	0.02	0.01	0.0	0.28	1.69
12a	LP Br	0.03	0.03	0.02	0.05	1.87
11a	LP Cl	0.13	0.10	0.05	1.33	0.40
10a	LP Cl	0.05	0.0	0.06	1.72	0.18
9a	C-(Cl, Br, F)	0.43	0.0	0.33	0.68	0.56
8a	C-(F, Cl, H)	0.45	0.21	0.61	0.58	0.15
7a	LP F / C-F	0.45	0.04	1.07	0.24	0.21
6a	LP F / C-F	0.24	0.0	1.50	0.18	0.08
5a	C-F, C-H	0.62	0.18	1.13	0.05	0.02
4a	C-H, C-F	0.60	0.20	0.55	0.26	0.39
3a	C-Br	0.26	0.02	0.05	0.37	1.30
2a	C-Cl	0.46	0.03	0.08	1.28	0.14
1a	C-F	0.15	0.01	1.82	0.01	0.01

Table 4

Calculated (HF, ADC(3) and nD-ADC(3) methods, basis set aug-cc-pVDZ) energies (E, eV) and intensities (P) of the most intense vertical valence shell ionization transitions in bromochlorofluoromethane in comparison with experimental results

Molecular orbital	Theory					Experiment	
	HF	ADC(3)		nD-ADC (3)		Present <sup>a</sup>	Novak et al [5]
	E	E	P	E	P	E	E
13a	11.76	11.12	0.91	11.07	0.91	11.15	11.16±0.03
12a	11.98	11.34	0.91	11.29	0.91	11.43	11.49±0.03
11a	12.81	12.02	0.90	11.96	0.91	12.02	12.05±0.01
10a	13.46	12.59	0.90	12.52	0.90	12.62	12.60±0.03
9a	15.07	14.12	0.90	14.05	0.90	13.98	14.02±0.03
8a	16.22	14.82	0.89	14.74	0.89	14.46	14.47±0.03
7a	19.55	17.69	0.09	17.57	0.07	} 17.5	} 17.56±0.05
6a	20.09	17.77	0.10	17.67	0.38		
		17.81	0.66	17.73	0.37		
		18.04	0.83	17.95	0.82		
5a	21.17	19.27	0.58	19.19	0.58	} 18.6	} 18.7±0.1
			0.24	19.21	0.22		
			0.05	19.30	0.05		

<sup>a</sup> The experimental uncertainty is ~0.03 eV

Table 5

Vertical outer valence ionization energies (eV) of bromochlorofluoromethane calculated using the OVGf scheme and different basis sets

Molecular orbital	cc-pVDZ	aug-cc-pVDZ	cc-pVTZ	aug-cc-pVTZ	cc-pVQZ	aug-cc-pVQZ	cc-pV5Z	6-311G**	6-311++G**
13a	10.96	11.16	11.20	11.29	11.37	11.41	11.42	10.97	11.01
12a	11.18	11.39	11.42	11.51	11.60	11.63	11.64	11.18	11.23
11a	11.78	12.02	12.00	12.10	12.14	12.18	12.18	11.80	11.85
10a	12.34	12.59	12.58	12.68	12.72	12.77	12.77	12.34	12.40
9a	13.82	14.15	14.02	14.16	14.17	14.22	14.21	13.84	13.96
8a	14.54	14.90	14.75	14.89	14.89	14.95	14.94	14.57	14.71
7a	17.55	17.96	17.75	17.91	17.89	17.95	17.94	17.47	17.60

Table 6

Twelve lowest vertical ionization energies (eV) of bromochlorofluoromethane calculated using the SAC-CI(SDT)/cc-pVDZ and nD-ADC(3)/aug-cc-pVDZ schemes in comparison with the experimental results

Molecular Orbital	SAC-CI(SDT)	nD-ADC(3)	Present <sup>a</sup>	Peak
13a	10.86	11.07	11.15	A <sub>1</sub>
12a	11.09	11.29	11.43	A <sub>2</sub>
11a	11.76	11.96	12.02	B
10a	12.44	12.52	12.62	C
9a	13.83	14.05	13.98	D
8a	14.56	14.74	14.46	E
			15.8	F
7a	$\left\{ \begin{array}{l} 17.57 \\ 17.61 \\ 17.69 \\ 17.78 \\ 17.82 \end{array} \right.$	$\left\{ \begin{array}{l} 17.52 \\ 17.57 \\ 17.67 \\ 17.73 \\ 17.78 \end{array} \right.$	$\left. \begin{array}{l} \\ \\ \\ \\ \\ \end{array} \right\} 17.5$	G
6a	18.02	17.95		

<sup>a</sup> The experimental uncertainty is ~0.03 eV

## Figure captions

- Figure 1 Photoelectron spectra of bromochlorofluoromethane, recorded at photon energies of 20, 28 and 42 eV, for  $\theta=0^\circ$  (left hand frames) and  $\theta=90^\circ$  (right hand frames). At each photon energy, the relative photoelectron intensity at  $\theta=0^\circ$  is correctly normalised to that at  $\theta=90^\circ$ . The photoelectron asymmetry parameters for the principal bands are shown in the right hand frames. The molecular orbitals associated with the bands and the band labels (Table 1) are indicated in the left hand frames.
- Figure 2 The photoelectron spectrum of bromochlorofluoromethane recorded at a photon energy of 37 eV for  $\theta=0^\circ$  (a) and  $\theta=90^\circ$  (b). The molecular orbitals associated with the bands are indicated.
- Figure 3 (a) The valence shell photoelectron spectrum of bromochloro-fluoromethane recorded at a photon energy of 80 eV for  $\theta=0^\circ$ . (b) The theoretical photoelectron spectrum of bromochlorofluoromethane obtained using the ADC(3) method.